

Uncertainty Problem as Illustrated by Magnetotherapy

Przemyslaw Syrek

Department of Electrical and Power Engineering
AGH University of Science and Technology, Krakow, Poland
syrekp@agh.edu.pl

Abstract — This article presents the impact of fixed tissue conductivities on the distribution of eddy currents in human body. Electrical conductivities characterising human tissues present in limbs have been collated based on various publications from the last 25 years. The article shows the extent to which simulation results are affected by changes to electrical conductivity of specific tissues. It has been demonstrated that the tissues taking the largest part of the studied domain have the greatest impact. The conclusions from these results suggest that it is very important to determine the electrical conductivity of tissues forming the human body with increasing precision, as it is an important factor affecting the accuracy of results. This factor seems much more significant than the growth in the precision of models resulting from increasing resolution of numerical models made available for research purposes.

Index Terms — Bioelectromagnetics, eddy currents, other dielectric or magnetic materials, magnetic devices, magnetic fields, uncertainty problem.

I. INTRODUCTION

Magnetotherapy is a method of treatment or stimulation of human body tissues the current is induced by means of a time-varying magnetic component (Magnetic Field–MF) of Electromagnetic Field (EMF) and used in the treatment of many diseases [1]. Unlike the stressful method involving electrodes, magnetotherapy relies on induction of electric currents in the tissue without physical contact and is used especially in regard to bones [2], [3]. Calculation of the distribution of magnetic field-induced eddy currents in limbs require relatively high computational complexity. However, as computers are becoming more powerful, and virtual human models that involve systems of hundreds of thousands of equations to be solved are becoming available, the time necessary to carry out relevant calculations can be less than an hour, even if we use computers available to the general public (at a reasonable price). The driver for research, including numerical computations, is multifaceted work related to transcranial magnetic stimulation (TMS). This is the area

where solutions of very accurate models are being forced [4], which results in the necessity to solve systems of tens of millions of algebraic equations.

In addition to the tendency to increase the accuracy of calculations by compacting grids – resulting from the resolution of available models, sometimes it is necessary to use significantly simplified models, especially when devices are optimized, e.g., magnetic coils [5]. Then the field problem can be solved analytically or be reduced to calculate a curve integral [6] with a mathematical representation of a coil [7].

The growing accuracy of calculations, however, is still accompanied by some uncertainty. It is related to the electrical parameters of tissues, particularly their electrical conductivity. This article shows how significant for the analysis of eddy currents distribution is conductivity of specific tissues and how significantly it can impact the results. Based on the cited works, it has been shown that there are large discrepancies in tissue conductivity in computational models used in recent decades.

Although electrical parameters and publications on this subject have been appearing for several decades, in recent years, very high-resolution models of human body's structure have been developed. The article shows that, in contrast to the model's resolution, and three-dimensional mesh generation method, the tissues conductivities are very important, and may substantially affect the results – also those presented using statistical tools.

II. COMPUTATIONAL PROBLEM

A. Magnetotherapy background

Calculation of eddy currents distribution uses a model from Virtual Family [8], which is based on MRI scans of women (Ella): 26-year-old, 1.63 meters in height and over 58 kg in weight. The eddy currents distribution was evaluated in a 100 mm fragment of an upper limb (left arm), whose skeleton was shown in Fig. 1 in an X-Ray-like style. Calculations use a largely extended domain, i.e., nearly the entire arm from the humerus to the wrist. In the figure in question, three cross-sections (CS1, CS2, CS3) have been marked perpendicularly to both bones in this limb fragment.

Tissue distribution for these cross-sections have been shown in the subsequent illustrations: Figs. 2–4.

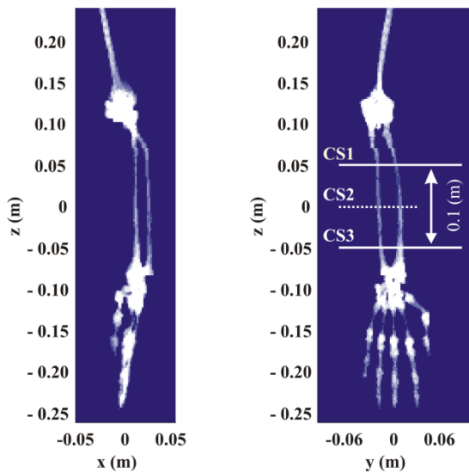


Fig. 1. The women's left hand. Cross sections (CS1, CS2, CS3) presented on next figures.

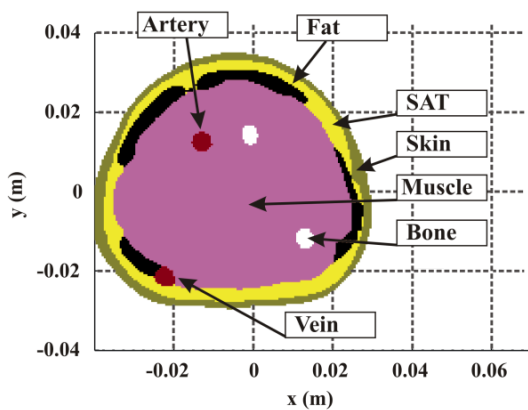


Fig. 2. Cross section CS1 and highlighted tissues. CS1 is an upper boundary of analysed domain.

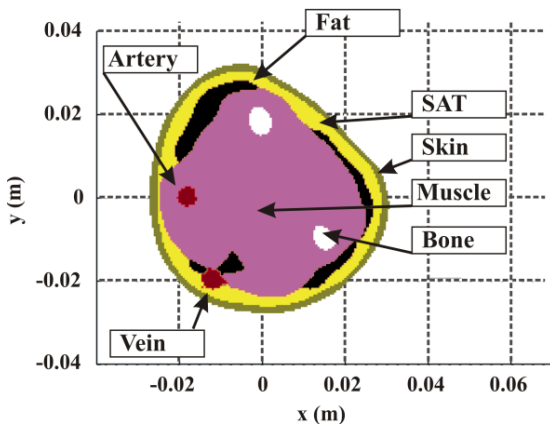


Fig. 3. Cross section CS2 and highlighted tissues.

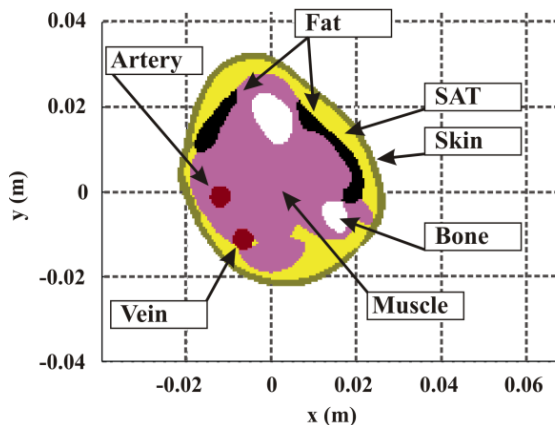


Fig. 4. Cross section CS3 and highlighted tissues. CS3 is a lower boundary of analysed domain.

This 100 (mm) limb fragment has the volume of nearly 276,000 cubic millimetres and is divided into sub-domains corresponding to 8 tissues present in them, which has been collated in Table 1. Data has been collated based on a model with the resolution of 1 mm. It also uses the Iso2mesh free library to overlay the tetrahedral mesh over the structural mesh [9] forming the border between both the arm and the air (insulator).

Table 1: Tissues in 100 mm part of the limb

Tissue	Volume (mm ³)	Percent of Total Volume (%)
All	275904	100.00
Muscle	168304	61.00
Subcutaneous adipose tissue (SAT)	45984	16.67
Skin	29608	10.73
Fat	22752	8.25
Bone	5072	1.84
Veins	2168	0.79
Arteries	1984	0.72
Marrow red	32	0.01

The simulations presented in the article use the coil with a multilayer solenoid (Fig. 5), 0.1 (m) in inner radius and 0.2 (m) in length (along the z-axis). The coil is powered with sinusoidal current whose RMS is equal to 1 (A). The axis of the main coil is parallel to and nearly coincides with the long bones of the upper limb, i.e. ulna and radius. Two bones positioned in such a way are extremely useful for this reflection, because a single long bone situated almost at the axis of symmetry of the domain in question could be located in such a manner, that eddy current paths would run around it regardless of its conductivity.

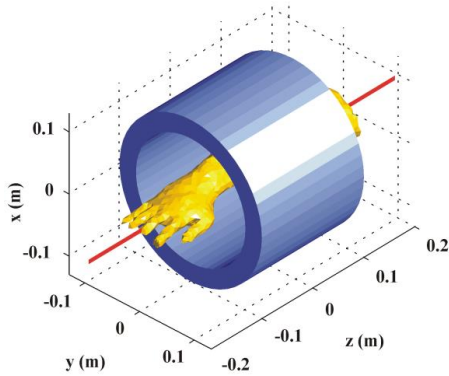


Fig. 5. Applicator, hand's model and z-axis.

The arm is exposed to a sinusoidal B-field of about 25 (mT) (RMS) at 50 (Hz). This coil is characterised by a relatively homogeneous B-field. The B-field distribution along the coil axis, is shown in Fig. 6.

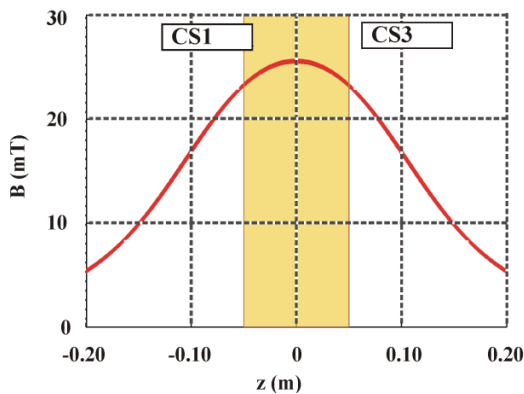


Fig. 6. Magnetic field with the x-axis.

B. Field model

Determining the current (here: eddy currents) density distribution using numerical methods requires the use of an appropriate model whose complexity depends on the type of problem being analysed. There is an assumption, that ferromagnetic materials are absent in the domain, and the entire domain is characterised by magnetic permeability equal to the magnetic constant. Due to the very low dielectric permittivity of human tissues and the air surrounding them, and due to the low frequency band, displacement current is neglected.

Human tissues are characterised by relatively low electrical conductivity as well, and in addition, the limb (body) is surrounded by air (an insulator of zero-conductivity). Hence, the eddy currents reach quite low values, and magnetic field induced by them (secondary magnetic field) it is insignificantly low in relation to the external field induced by the coil.

For this type of issues, the so-called AV model – a pair of: vector magnetic potential (A) and electrical

potential (V) – is provided. Thus, the analysed domain is described by the Partial Differential Equation (PDE), which is replaced by a system of algebraic equations. In turn, the equation system and its dimension depend on accuracy (resolution) of model used. Both PDE and Boundary Conditions, which are unavoidable in this case, have been introduced in: [10]–[12].

Thanks to the properties of the domain presented above, the results are scalable, since the model is linear in the extremely low frequency band. Once the eddy current distribution is determined for a given spatial configuration of the limb and the coil, this gives the option of converting the result using a real coefficient. It is assumed that the source (current of coil and MF distribution) is scaled by this coefficient. This was used to standardize the results obtained for a collective presentation.

C. Numerical solution procedure

To obtain the results, proper partial differential equation has to be replaced by system of algebraic (here linear) equations. For this purpose, Finite Element Method (FEM) with cubic elements was used. This kind of spatial mesh is due to geometry of human body model, composed of voxels. The analyzed problem involves formulation and solution of over 338 thousand of equations. To obtain one solution of PDE on personal computer with clock rate of 3.30 GHz and 16 GB of RAM, about one hour is needed.

The total computational time consists of several stages. The first is creation of matrix corresponding to the left side of equation system. This matrix is rare, and its exact structure and values of entries depend on mutual location of individual elements of human body model and their electrical properties. Matrix formulation takes about 2600 seconds (it is almost 44 minutes).

Right-hand side of equation system is generated on the basis of magnetic vector potential's distribution within the border of subareas of different electrical conductivities. This stage lasts over 180 seconds, mainly because of integration related to a generation of MF. In turn, the very solution of equation system takes about 82 seconds.

The generation of a cubic structural mesh, unlike non-fixed structure meshes (e.g., tetrahedral mesh), is not characterized by high computational complexity. Meshing itself, however, is inseparable from computational solutions of partial differential equations.

However, as long as optimization is not carried out, but rather an evaluation of several or dozen of material properties' combinations, this total time seems to be satisfactory.

III. SOURCE OF UNCERTAINTY

The analysis of tissue conductivities made available in publications released over the last two decades and

parameters adopted by the authors lead to large discrepancies – this applies to both conductors [13] and low conductivity materials [14, 15]. Table 2 collates conductivities provided in various publications, which are discussed and commented on below. The percentage volume of tissue stems from a specific 0.1 m fragment of a limb. Chapter has been divided into 6 parts corresponding to respective columns of Table 2. Apart from the references to the literature, points below include some comments related to the more or less accurate characteristics of particular tissues.

1) Conductivity σ_1 collated in the table based on [16]; according to Scopus - database, this article was cited over 1900 times. The authors distinguish between two types of bone structure: cortical and cancellous. A number of articles cite results shown in that article, particularly for magnetotherapy simulation [17]. It is also worth noticing that electrical conductivity may to a smaller or greater extent vary with the frequency, also within a narrow band up to 1000 (Hz) [18]. Some tissues, such as muscle, also show anisotropy.

2) Conductivity σ_2 in the table was proposed on the basis of [19], which used the data from [20].

3) Article [21] sets together mean values of tissues conductivities on the basis of [22] – supplemented in the table as σ_3 . [23] refers to the mean value from multiple references and bone tissue is adopted by them on the level of 0.010 (S/m).

4) The sinusoidal low frequency stimulation with varying magnetic component of EMF, at the frequency of 50 (Hz), is relatively compatible to models used in Transcranial Magnetic Stimulation (TMS) and Spinal Cord Stimulation, in relation to a tissue electrical conductivity. After the query of this topic, the table

contains next column, due to conductivity values collected in [24], [25]. It is shown as σ_4 .

5) In research [26] presents the σ_5 list of conductivities, clearly marking that the skin is treated as a composite tissue consisting of skin proper and subcutaneous fat (SAT). The above points show how complicated this problem is. Only some sources distinguish between skin and the subcutaneous adipose tissue (SAT).

6) In [27], authors collate data shown here as the σ_6 list. The article deals with calculation for an Extremely Low Frequency, namely 60 (Hz).

Further reflection is based on two different conductivity values for important tissues. The primary tissue chosen for the discussion is the muscular tissue, whose impact on the induction of eddy currents in a variable magnetic field is the greatest due to its large volume. Another significant conductivity is related to the bone tissue, due to the fact that magnetotherapy is used especially for bone injury treatment. Moreover, two conductivities were considered for subcutaneous adipose tissue (SAT), fat and skin tissue. Here, for the sake of the need to preserve transparency of the results, conductivities assigned to those tissues were identical in each variant, hence the subscripts (SFS) refer to data related to the three tissues. Fortunately, for the frequencies used in magneto therapy, dependencies between frequency and tissue conductivity do not exist in contrast to other form of therapy [28], and this factor may be omitted.

Without discussing the validity of the adopted tissue conductivities, the impact of specific parameters on the results will be shown with particular emphasis on currents induced in bones.

Table 2: Tissues electrical conductivities

Tissue	σ_1 (S/m)	σ_2 (S/m)	σ_3 (S/m)	σ_4 (S/m)	σ_5 (S/m)	σ_6 (S/m)
Muscle	0.241	0.202	0.150	0.160	0.350	0.233
SAT (subcutaneous adipose tissues)	–	0.012	–	0.078	–	–
Fat	0.020	0.012	0.078	0.078	0.040	–
Skin	0.0002	0.012	–	0.100	0.100	–
Veins and arteries	–	–	–	–	–	0.700
Blood vessel	0.264	0.700	0.600	0.600	0.700	–
Bone	–	0.020	–	0.015	0.020	0.050
Bone (cortical)	0.020	–	–	–	–	–
Bone (cancellous)	0.081	–	–	–	–	–
Bone (trabecular)	–	–	–	–	0.070	–

IV. RESULTS

A. Evaluation criteria

The maximum value in the analysed domain should be examined first. According to [29] and cited previously [11], the 99th percentile (A99) is used to avoid computational instabilities instead of maximum result from analysed domain. And the introduced A50 factor,

corresponds to a median value of current within the analysed area. Other symbols for factors are formed by combining the first letter (or letters) of the name of the tissue and the percentile. These are: A – for all tissues considered together, M – for muscle tissue, B – for bone, SAT – for subcutaneous adipose tissue, Fat – for fat tissue and Skin – for skin. The 50th percentile (median)

and, in the case of the most important tissues, the 99th percentile are highlighted. It refers to a muscles, characterised by relatively high conductivity, and since the muscles take the most space within the examined domain. The second is bone tissue, and this results from the fact that this tissue is treated using magnetotherapy.

B. Exemplary results

For the coil in question, whose MF reaches 25 (mT) along the axis, and $\sigma_{MUSCLE}=0.350$ (S/m), $\sigma_{SFS}=0.078$ (S/m) (common conductivity for: subcutaneous adipose tissue (SAT), fat and skin), $\sigma_{BONE}=0.050$ (S/m), the results have been shown in Table 3.

Table 3: Exemplary results

Factor	J (mA/m ²)
A99	36.86
A50	12.94
M99	37.08
M50	20.06
B99	11.24
B50	6.56
SAT50	8.69
Fat50	8.73
Skin50	6.15

The results, particularly A99, lead to the conclusion that the MF and the assumed tissue conductivities (the highest ones among the considered values) do not produce results that might lead to a risk of bodily injury. As stated by [30], this level should not exceed 100 (mA/m²).

Table 4: Tissues electrical conductivities. Results for all combinations of selected tissue conductivities (A99 is 10 mA/m²)

σ_{MUSCLE}	σ_{SFS}	σ_{BONE}	A50	M99	M50	B99	B50	SAT50	Fat50	Skin50
0.350	0.078	0.050	3.510	10.058	5.441	3.049	1.781	2.356	2.367	1.668
0.350	0.078	0.015	3.440	10.085	5.331	1.239	0.643	2.331	2.332	1.655
0.350	0.012	0.050	3.084	10.178	5.003	3.023	1.645	0.352	0.367	0.241
0.350	0.012	0.015	3.047	10.203	4.950	1.175	0.563	0.346	0.364	0.239
0.160	0.078	0.050	4.551	8.908	5.182	4.425	2.838	4.443	4.233	3.247
0.160	0.078	0.015	4.265	8.503	4.839	1.940	1.097	4.171	3.931	3.049
0.160	0.012	0.050	3.030	9.583	4.809	4.531	2.657	0.723	0.743	0.499
0.160	0.012	0.015	2.928	9.470	4.708	2.150	1.105	0.712	0.724	0.492

The mutual relations between conductivities of tissues significantly impact the possibility to achieve highest currents in bones undergoing treatment, as

Further reflection, involving various conductivities adopted for specific tissues, the results will be scaled to adjust the A99-factor to a value equal to 10 (mA/m²) for the sake of greater clarity.

C. Impact of tissue properties on results

Table 4 shows the results for various tissue conductivities. In the fourth and fifth row of results, it can be seen that M50 is nearly equal to 60% of M99, unlike other cases, where it is merely 50%.

These two cases occur when combining lower conductivity for muscles with higher conductivity of SFS (SAT, fat, skin). This is confirmed by the fact, that the analysed domain, a set of tissues, jointly form eddy current paths, and the parameters of individual tissues do not directly translate into the results.

What can seem surprising is the fact, that the highest result for B50 (fifth row in Table 4) was achieved with low conductivity of muscles surrounding the bone. It is also worth stressing that lower conductivity of muscles, due to the fact that they form the majority of limb volume, significantly reduces A99 throughout the limb, which allows the MF to be set at a level not posing a risk to the tissues, and hence achieve much higher B50 levels. Furthermore, with the same fixed conductivities for muscles and SFS, B50 results preserve the proportion corresponding the ratio of the fixed conductivities for bone tissue itself (rows 1 and 2 and subsequent pairs of rows in the B50 column of Table 4). The change (by over three times) of the fixed bone conductivity in turn causes minimum fluctuations of results for all the remaining tissues, which results from the very low volume taken by bone tissue compared to the entire domain.

shown in Fig. 7 and Fig. 8. Eddy currents must always be concentrated in bone tissue with consideration to safe levels in other tissues.

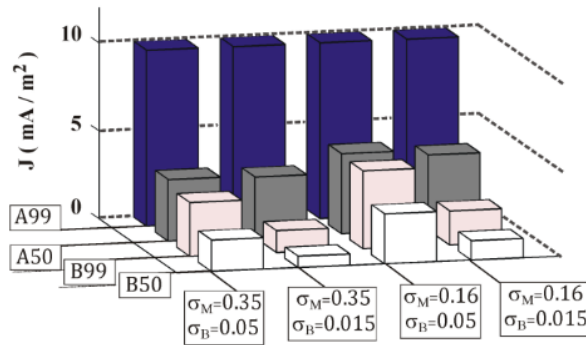


Fig. 7. Current densities factors (A99, A50, B99, B50) for $\sigma_{SFS} = 0.078$ (S/m).

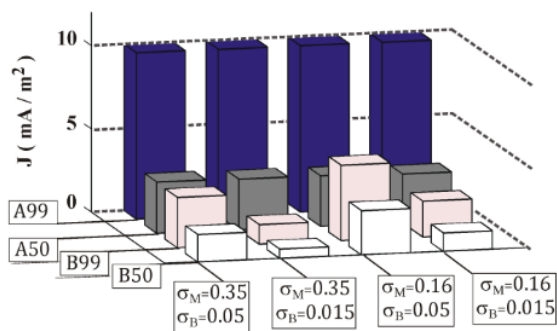


Fig. 8. Current densities factors (A99, A50, B99, B50) for $\sigma_{SFS} = 0.012$ (S/m).

V. CONCLUSIONS

Each organism might differ in size, which affects eddy current paths. Moreover, the percentage of specific tissues can vary depending on the fact content and other factors. As shown here, another factor contributing to the uncertainty of what human body tissues are exposed to, is the real conductivity characterising the tissues. While analysis the eddy current density distribution in human body, there is a need to decide what parameters should be assigned to specific tissues. As shown above, there are many options to choose from, and this decision can significantly influence the results achieved using the same device whose work is simulated in compliance with certain absolute allowed current levels. Virtual human models available for numerical investigations [31], [32] are becoming more numerous and more precise. Based on the results presented here, however, it can be observed, that despite the achievements of recent decades, it is very important to carry out further research to identify accurate and unambiguous parameters, particularly electrical conductivity of specific tissues.

REFERENCES

[1] D. Andritoi, V. David, and R. Ciorap, "Dynamics analysis of heart rate during magneto-therapy

session," *2014 International Conference and Exposition on Electrical and Power Engineering (EPE)*, Iasi, pp. 514-517, 2014.

- [2] S. M. Schwab, C. Androjna, E. I. Waldorff, J. T. Ryaby, L. R. Moore, R. J. Midura, and M. Zborowski, "Mechanical stress on suspended cortical bone sample by low frequency magnetic field," *IEEE Transactions on Magnetics*, vol. 52, no. 7, pp. 1-4, 2016.
- [3] A. Miaskowski, A. Krawczyk, and Y. Ishihara, "A numerical evaluation of eddy currents distribution in the human knee with metallic implant," *COMPEL: The International Journal for Computation and Mathematics in Electrical and Electronic Engineering*, vol. 31, no. 5, pp. 1441-1447, 2010.
- [4] P. I. Petrov, S. Mandija, I. Sommer, C. van den Berg, and S. Neggers, "How much detail is needed in modeling a transcranial magnetic stimulation figure-8 coil: Measurements and brain simulations," *PLoS ONE*, vol. 12, no. 6, pp. 1-20, 2017.
- [5] B. Minnaert, L. De Strycker, and N. Stevens, "Design of a planar, concentric coil for the generation of a homogeneous vertical magnetic field distribution," *ACES Journal*, vol. 32, no. 12, pp. 1056-1063, 2017.
- [6] G. M. Noetscher, S. N. Makarov, F. Sciré-Scappuzzo, and A. Pascual-Leone, "A simple absolute estimate of peak eddy currents induced by transcranial magnetic stimulation using the GR model," *IEEE Transactions on Magnetics*, vol. 49, no. 9, pp. 4999-5003, 2013.
- [7] P. Syrek and R. Barbulescu, "Parametric curves to trace the TMS coils windings," *10th International Symposium on Advanced Topics in Electrical Engineering (ATEE)*, Bucharest, Romania, pp. 386-391, 2017.
- [8] A. Christ, W. Kainz, E. G. Hahn, K. Honegger, M. Zefferer, E. Neufeld, W. Rascher, R. Janka, W. Bautz, J. Chen, B. Kiefer, P. Schmitt, H. P. Hollenbach, J. X. Shen, M. Oberle, D. Szczerba, A. Kam, J. W. Guag, and N. Kuster, "The virtual family – development of surface-based anatomical models of two adults and two children for dosimetric simulations," *Physics in Medicine and Biology*, vol. 55, no. 2, pp. 23-38, 2010.
- [9] Q. Fang and D. Boas, "Tetrahedral mesh generation from volumetric binary and gray-scale images," *Proceedings of IEEE International Symposium on Biomedical Imaging*, pp. 1142-1145, 2009.
- [10] G. M. Noetscher, S. N. Makarov, F. Sciré-Scappuzzo, and A. Pascual-Leone, "A simple absolute estimate of peak eddy currents induced by transcranial magnetic stimulation using the GR model," *IEEE Transactions on Magnetics*, vol. 49, no. 9, pp. 4999-5003, 2013.

- [11] V. Guadagnin, M. Parazzini, S. Fiocchi, I. Liorni, and P. Ravazzani, "Deep transcranial magnetic stimulation: modeling of different coil configurations," *IEEE Transactions on Biomedical Engineering*, vol. 63, no. 7, pp. 1543-1550, 2016.
- [12] S. N. Makarov, J. Yanamadala, M. W. Piazza, A. M. Helderman, N. S. Thang, E. H. Burnham, and A. Pascual-Leone, "Preliminary upper estimate of peak currents in transcranial magnetic stimulation at distant locations from a TMS coil," *IEEE Transactions on Biomedical Engineering*, vol. 63, no. 9, pp. 1944-1955, 2016.
- [13] S. Lall  ch  re, "Advanced statistical 3D models of composite materials for microwave electromagnetic compatibility applications," *ACES Journal*, vol. 32, no. 12, pp. 1113-1116, 2017.
- [14] G. Liu, "Time-domain electromagnetic inversion technique for biological tissues by reconstructing distributions of cole-cole model parameters," *ACES Journal*, vol. 32, no.1, pp. 8-14, 2017.
- [15] P. Gas, "Optimization of multi-slot coaxial antennas for microwave thermotherapy based on the S11-parameter analysis," *Biocybernetics and Biomedical Engineering*, vol. 37, no.1, pp. 78-93, 2017.
- [16] S. Gabriel, R. W. Lau, and C. Gabriel, "The dielectric properties of biological tissues: III. Parametric models for the dielectric spectrum of tissues," *Physics in Medicine & Biology*, vol. 41, no. 11, pp. 2271-2293, 1996.
- [17] A. Miaskowski, A. Krawczyk, and Y. Ishihara, "Computer modelling of magnetotherapy in orthopedic treatments," *COMPEL: The International Journal for Computation and Mathematics in Electrical and Electronic Engineering*, vol. 29, no. 4, pp. 1015-1021, 2010.
- [18] A. Bouazizi, G. Zaibi, M. Samet, and A. Kachouri, "Parametric study on the dielectric properties of biological tissues," *16th International Conference on Sciences and Techniques of Automatic Control and Computer Engineering (STA)*, Monastir, pp. 54-57, 2015.
- [19] M. Parazzini, S. Fiocchi, I. Liorni, and P. Ravazzani, "Effect of the interindividual variability on computational modeling of transcranial direct current stimulation," *Computational Intelligence and Neuroscience*, vol. 2015, Article ID 963293, pp. 1-9, 2015.
- [20] NRCalfAP 2015, National Research Council and Institute for Applied Physics, "Nello Carrara", "An internet resource for the calculation of the dielectric properties of body tissues," *IFAC-CNR, Florence, Italy*. <http://niremf.ifac.cnr.it/tissprop/>, 2015.
- [21] B. Sawicki and A. Krupa, "Experiments with models of variability for biological tissues," *Przegl  d Elektrotechniczny*, vol. 92, no. 7, pp. 83-86, 2016.
- [22] C. Gabriel, A. Peyman, and E. H. Grant, "Electrical conductivity of tissue at frequencies below 1 MHz," *Physics in Medicine & Biology*, vol. 54, no. 16, pp. 4863-4878, 2009.
- [23] T. A. Wagner, M. Zahn, A. J. Grodzinsky, and A. Pascual-Leone, "Three-dimensional head model simulation of transcranial magnetic stimulation," *IEEE Transactions on Biomedical Engineering*, vol. 51, no. 9, pp. 1586-1598, 2004.
- [24] M. Parazzini, S. Fiocchi, I. Liorni, E. Rossi, F. Cogiamanian, M. Vergari, A. Priori, and P. Ravazzani, "Modeling the current density generated by transcutaneous spinal direct current stimulation (tsDCS)," *Clinical Neurophysiology*, vol. 125, no. 11, pp. 2260-2270, 2014.
- [25] M. Parazzini, S. Fiocchi, A. Cancelli, C. Cottone, I. Liorni, and P. Ravazzani, "A computational model of the electric field distribution due to regional personalized or nonpersonalized electrodes to select transcranial electric stimulation target," *IEEE Transactions on Biomedical Engineering*, vol. 64, no. 1, pp. 184-195, 2017.
- [26] P. Dimbylow, "Development of the female voxel phantom, NAOMI, and its application to calculations of induced current densities and electric fields from applied low frequency magnetic and electric fields," *Physics in Medicine and Biology*, vol. 50, pp. 1047-1070, 2005.
- [27] L. H. Hoang, R. Scorretti, N. Burais, and D. Voyer, "Numerical dosimetry of induced phenomena in the human body by a three-phase power line," *IEEE Transactions on Magnetics*, vol. 45, no. 3, pp. 1666-1669, 2009.
- [28] P. Gas and A. Miaskowski, "SAR optimization for multi-dipole antenna array with regard to local hyperthermia," *Przegl  d Elektrotechniczny*, vol. 95, no. 1, pp. 17-20, 2019.
- [29] M. Parazzini, S. Fiocchi, and P. Ravazzani, "Electric field and current density distribution in an anatomical head model during transcranial direct current stimulation for tinnitus treatment," *Bioelectromagnetics*, vol. 33, no. 6, pp. 476-487, 2012.
- [30] ICNIRP 2010, "Guidelines for limiting exposure to time-varying electric and magnetic fields (1 Hz–100 kHz)," *Health Physics*, vol. 99, no. 6, pp. 818-836, 2010.
- [31] S. N. Makarov, G. M. Noetscher, J. Yanamadala, M. W. Piazza, S. Louie, A. Prokop, A. Nazarian, and A. Nummenmaa, "Virtual human models for electromagnetic studies and their applications," *IEEE Reviews in Biomedical Engineering*, vol. 10, pp. 95-121, 2017.
- [32] P. C. Miranda, R. Salvador, C. Wenger, and S. R. Fernandes, "Computational models of non-invasive brain and spinal cord stimulation," 2016

38th Annual International Conference of the IEEE Engineering in Medicine and Biology Society (EMBC), Orlando, FL, pp. 6457-6460, 2016.



Przemyslaw Syrek received his Master Degree in Electrical Engineering in 2005 and Ph.D. in the same area from AGH University of Science and Technology in Krakow, Poland (2011), where he has been working in Department of Electrical and Power Engineering. His major research interest is field theory, including biomedical applications of electromagnetic field.